Sustainable Cities and Society 41 (2018) 907–918

Contents lists available at ScienceDirect

Sustainable Cities and Society

journal homepage: www.elsevier.com/locate/scs

Assessing urban water security under changing climate: Challenges and ways forward

Pablo Jaramillo, Ali Nazemi*

Department of Building, Civil and Environmental Engineering, Concordia University, Montreal, Quebec, Canada

ARTICLE INFO

Keywords:
Urban water security
Climate change impact assessment
Downscaled climate simulations
Spatiotemporal climate variability and change
Modeling uncertainty
Montreal, Quebec

ABSTRACT

Climate change has altered the elements of water availability, water demand and climate extremes in time and space. Such changes have various implications on water security, particularly in urban regions that are highly concentrated with human population and socio-economic activities. Assessing the climate change impacts on water security is often based on using the projections from an ensemble of climate models which are further downscaled into finer spatial resolutions. The availability of downscaled climate simulations has resulted in the optimism that future climate change threats to urban water security could now be quantified at the scale of individual cities; however, is this really the case? To showcase some of the challenges in the direct application of downscaled climate projections for impact assessment, here we explore the reliability of a state-of-the-art ensemble of downscaled climate simulations in the city of Montreal, Canada. We show that spatial variability in long-term climate over Montreal is misrepresented by downscaled climate projections. In addition, uncertainty in future projections as a result of climate models and/or concentration pathways can pose extra challenges in application of the downscaled projection in real-world design and operational contexts. Based on the currently available literature, we suggest few directions to handle current modeling uncertainties until improved climate modeling technology becomes available.

1. Introduction

Being home to more than 50% of the world's population, urban areas now represent the highest concentration of human population and socio-economic activities globally (Ibrahim, Sugar, Hoornweg, & Kennedy, 2012; Seto, Güneralp, & Hutyra, 2012; Seto, Sánchez-Rodríguez, & Fragkias, 2010). As water is prominent to human life and development, protecting human societies against adverse effects of water scarcity and surplus is central focus in water security (Wheater & Gober, 2013, 2015). Addressing water security in urban landscapes, however, is inherently complex. This is due to massively coupled relationships between water and human systems, which dynamically change across various temporal and spatial scales (see e.g. Chang, Praskievicz, & Parandvash, 2014; House-Peters & Chang, 2011; Parandvash & Chang, 2016). Most importantly, highly concentrated human activities initiate a large amount of water demand that requires a continuous supply, often with high management priority (Gleick, 2003; Nkomo & van der Zaag, 2004). Nonetheless, quantifying water demand in urban areas is not an easy task as it involves a highly varying interplay between climate, land and hydrological conditions in conjunction with details of socio-economy and technological developments (Breyer, Chang, & Parandvash, 2012; Franczyk & Chang, 2009; Ghiassi, Zimbra, & Saidane, 2008; Kenney, Goemans, Klein, Lowrey, & Reidy, 2008; Praskievicz & Chang, 2009). In addition, urban infrastructures are highly prone to extreme weather conditions, such as heavy precipitations, that can translate into severe floods (e.g., Barroca, Bernardara, Mouchel, & Hubert, 2006; Huong & Pathirana, 2013; Smith & Handmer, 1984) and result in large economic consequences (e.g., Pomeroy, Stewart, & Whitfield, 2016; Wake, 2013). Having said that, the resulting vulnerabilities are not only dependent on the climate but are also largely determined by the land management and socio-economic development within the urban areas (Chen, Zhou, Zhang, Du, & Zhou, 2015; Hollis, 1975).

During the current *Anthropocene* (see Crutzen, 2006; Steffen, Grinevald, Crutzen, & McNeill, 2011), coupled natural-human systems are highly threatened due to ever-increasing changes in both human and natural systems (Steffen, Crutzen, & McNeill, 2007; Steffen, Persson, et al., 2011). In the context of urban water security, growing population and socio-economic activities has continuously increased both water demands and vulnerability to droughts and floods in urban areas (e.g. Cutter, 1996; Hallegatte, Green, Nicholls, & Corfee-Morlot, 2013; Hanasaki et al., 2013; Hejazi et al., 2014; Mokrech et al., 2015). In addition, climate change has perturbed the elements of water cycle and affected both water availability (McDonald et al., 2011;

* Corresponding author.
E-mail address: ali.nazemi@concordia.ca (A. Nazemi).

http://dx.doi.org/10.1016/j.scs.2017.04.005
Received 30 November 2016; Received in revised form 10 April 2017; Accepted 13 April 2017
Available online 19 April 2017

Vörösmarty, Green, Salisbury, & Lammers, 2000) and water demand (Hanasaki et al., 2013; Hejazi et al., 2014). On one hand, changes in form and magnitude of precipitation affected local water availability, which can be an important source of supply, particularly for a number of urban water demands such as watering green areas (e.g., Daniel, Lemonsu, & Viguié, 2016). On the other hand, it is known that warmer climate can increase municipal water use, particularly consumptive uses, due to the direct effect on the evapotranspiration (e.g., Parkinson et al., 2016). In addition, climate change-induced alterations in extreme precipitation pose extra vulnerability to urban water security, as the magnitude, duration and frequency of extreme rainfall events are directly linked to the design of urban infrastructures, such as storm water management systems (e.g., Mirhosseini, Srivastava, & Stefanova, 2013; Rodríguez et al., 2014; Schreider, Smith, & Jakeman, 2000; Simonovic, Schardong, & Sandink, 2016).

Addressing water security in the era of climate change, therefore, requires a careful attention to the alterations of relevant hydroclimate variables and how they can affect urban water security by changing the interactions within the coupled human–water systems. According to the general "top-down" climate change impact assessment framework, this essentially requires a predictive capability to identify the implications of climate change on the urban water resource management, with a greater goal of highlighting operational thresholds for accommodating future water demands and/or staying resilient against climate-induced hazards. Various models have been already proposed to quantify the impact of climate along with other influencing variables on urban water demand and/or water-related natural hazards. These models are either in the sense of standalone assessment tools (see Chang et al., 2014 for a number of examples) or as part of larger socio-economic (Hejazi, Edmonds, Chaturvedi, Davies, & Eom, 2013; Hejazi et al., 2014) and/or Earth System models (Nazemi & Wheater, 2015a, 2015b). Regardless of the context and/or predicting capability, the application of impact models for understanding future water security threats requires the availability of high-quality climate projections that can portray likely climate futures at the appropriate scale, relevant to forcing impact models. These projections should not only represent the temporal changes in climate variables, but should be also able to adequately represent the spatial variability in climate over urban areas.

The advent of publically available climate projections produced by the Intergovernmental Panel on Climate Change's 5th Coupled Model Intercomparison Project (IPCC-CMIP5; see IPCC, 2014; Taylor, Stouffer, & Meehl, 2012) provides the scientific basis to account for the effects of climate change globally. These projections have been recently coupled with various downscaling schemes (e.g., Harding, Snyder, & Liess, 2013; Timm, Giambelluca, & Diaz, 2015) to provide the data support required for quantifying climate change impacts at local to regional scales (e.g., Mearns et al., 2013; Thrasher et al., 2013). However, there is still no formal evaluation on whether the available downscaled climate projections can be readily used for addressing the impact of climate change in urban areas, for which capturing both spatial and temporal variability in climate variables has a prime importance. This obviously requires a body of benchmarking studies to inspect the reliability of available downscaled products across various urban regions throughout the globe. This is yet to appear; however, to demonstrate potential complications in direct applications of downscaled simulations in the context of urban design and management, we provide a general notion of reliability for a state-of-the-art ensemble of downscaled climate simulations at the Greater Montreal area and the neighboring region in Quebec, Canada. We look at how downscaled climate simulations can reproduce the observed long-term evolutions in a suite of annual climate variables that have relevance to urban water security in Montreal. It should be noted that we performed the same study at finer seasonal and monthly scales; however, we only report our results in the annual time scale for the sake of brevity and the fact that similar issues have been identified at finer time scales. As a result, the analysis of annual data can lead us to the identification of key sources of uncertainty in existing downscaled climate simulations in our case study. By looking at the prospective climate model simulations, we also provide a comprehensive view on wide ranges of projected changes in future hydroclimate variables as a result of different climate models and/or concentration pathways. By focusing on a real-world engineering design example, we then discuss how spatial variability and local uncertainty can lead into complexities for decision making. Accordingly, we suggest few directions to handle these obstacles until improved predictive climate modeling capability becomes available.

2. Case study

City of Montreal, referred to as "Canada's Cultural Capital", is a major urban center in southern Quebec. Being home to around 4 million people, the 4259 km^2 Greater Montreal is the second most populous region in the country (Statistic Canada, 2012) and the second-largest economy of Canadian cities based on GDP (Brown & Rispoli, 2014). Montreal has a humid continental climate. Annual total precipitation is around 1000 mm per unit of area, for which about one fourth is in the form of winter snowfall. Summers are warm and humid and maximum daily temperature can exceed 30 °C. Conversely, winter brings cold weather with minimum daily temperature falling below −20 °C for several days during the season. Spring and fall are mild but prone to drastic temperature swings and extreme precipitation events, with thunderstorms being common in late spring to early fall (see Environment Canada, 1987).

Key socio-economic sectors in the city includes high-tech and service industries, higher education, as well as business and finance (see Ville de Montreal, 2002), all requiring secure water and electrical energy supply for day-to-day operations. There is a strong nexus between water and energy in the city as the hydroelectric power supply is the main energy source in the province (CBC, 30 March 2011). Municipal water supply is provided by the water stored at lac Saint-Louis, lac des Deux-Montagnes, Rivière des Prairies as well as the St. Lawrence River. This water is then treated in seven plants with the total capacity of around 3 million cubic meters per day (see http://ville.montreal.qc.ca/portal/page?_pageid=6497,54201575&_dad=portal&_schema=PORTAL). The treated water is then distributed through water mains to the end users. The water distribution network is old, ranging between 83 to 123 years of age in some areas of the city, and several bursting incidents have taken place in recent years due to various reasons, including extreme temperature swings (Riga, 12 January 2016). The city has been also prone to flooding, most notably during the deadly flood of July 14, 1987 that caused by overwhelmed sewer systems, unable to carry the extreme rainfall in parts of the city.

3. Available data

We considered the Greater Montreal and its surrounding 25 km neighboring regions that strongly links to the city in terms of water and energy security. This forms a grid box with the total area of 12,500 km^2, which still stays in the sub-grid resolution of majority of IPCC-CMIP5 models (see https://verc.enes.org/data/enes-model-data/cmip5/resolution). Within this region, there are eight climate stations with complete historical record at the daily scale going back to 1950 – see Table 1 for a brief description of the climate stations. Daily climate data in these stations are available through Environment and Climate Change Canada (ECCC)'s National Climate Archive. The considered stations are homogeneous in terms of the elevation, with an exception of St. Jerome being the only station with the elevation more than 100 m above the sea level. Having said that, no significant orographic effect was noted as St. Jerome shows strong correlation and insignificant deviation from the three nearby gauges located in lower altitudes. Here we used the climate information at these stations as the ground truth for inspecting the reliability of the available downscaled climate simulations.

Table 1
Description of the eight climate stations used in this study.

ECCC ID	Name	Latitude	Longitude	Altitude (m)
7014160	L'ASSOMPTION	45°48′34.000″ N	73°26′05.000″ W	21.00
7014290	LES CEDRES	45°18′00.000″ N	74°03′00.000″ W	47.20
7015730	OKA	45°30′00.000″ N	74°04′00.000″ W	91.40
7023240	HUNTINGDON	45°03′00.000″ N	74°10′00.000″ W	49.10
7025250	MONTREAL/ P. TRUDEAU INTL A	45°28′00.000″ N	73°45′00.000″ W	32.10
7026040	PHILIPSBURG	45°02′00.000″ N	73°05′00.000″ W	53.30
7027320	MONTREAL/ ST-HUBERT A	45°31′00.000″ N	73°25′00.000″ W	27.40
7037400	ST JEROME	45°48′00.000″ N	74°03′00.000″ W	169.50

National Aeronautics and Space Administration (NASA) has recently downscaled historical and future daily minimum and maximum temperature and precipitation simulations of 21 IPCC-CMIP5 models into a unique spatial resolution of 0.25° × 0.25° globally – see Table 2 for the list of models used in this downscaled product. The downscaling is based on applying the widely-used Bias-Correction Spatial Disaggregation method (BCSD; see e.g., Thrasher, Maurer, McKellar, & Duffy, 2012; Wood, Leung, Sridhar, & Lettenmaier, 2004), using the observed gridded climate data product provided by Sheffield, Goteti, and Wood (2006). This multi-model downscaled data product is publically available through NASA's Earth Exchange Global Daily Downscaled Projections (NEX-GDDP; see the link to the data source in the Acknowledgment). The considered region for the Greater Montreal includes 20 grids with 0.25° × 0.25° resolution, in which daily retrospective downscaled climate data as well as the ground-based observations are available from 1950 to 2005. See Fig. 1 for the box region of the Greater Montreal covered by the 20 NEX-GDDP grids and the eight considered climate stations. The downscaled product also includes prospective runs from 2006 to 2099, which are used to provide insights about the future climate in the region. Prospective projections are obtained under two of the four greenhouse gas emissions scenarios (i.e. 4.5 and 8.5) known as Representative Concentration Pathways (RCPs; Meinshausen et al., 2011).

4. Methodology

4.1. Selected hydroclimate variables

We focused on nine annual hydroclimate variables that have relevance to water and energy security in the Greater Montreal and surrounding regions – see Table 3. We included energy-related variables because hydroelectricity, as noted above, is the main source of energy in the city and therefore there is a strong nexus between water and energy supply and use. These variables together provide proxies for water and energy demands, local water availability, seasonality in climate, as well as some extreme climate events that have implications on water and energy security.

In brief, minimum and maximum daily temperatures affect the range of daily consumptive water and energy demands (Guhathakurta & Gober, 2007; Maidment, Miaou, & Crawford, 1985). As a result, annual minimum and maximum daily temperatures can provide a proxy for expected range of water and energy demands throughout a year. Similarly, annually-averaged daily precipitation can provide a proxy for expected daily local water availability throughout a given year. The days with average temperature of zero or less can distinguish the form of precipitation from rain to snow, which determine the type of hydrologic response, i.e. snow accumulation vs. runoff. In addition, Annual Maximum Precipitation can provide a notion for extreme precipitation events that can translate into urban floods. Extreme warm periods are associated with both higher water and cooling energy consumptions (Bougadis, Adamowski, & Diduch, 2005; Colombo, Etkin, & Karney, 1999; Iglesias, Garrote, Diz, Schlickenrieder, & Martin-Carrasco, 2011; Lewis, 2011; Tewathia, 2014; Tian et al., 2016). In addition in cold-regions such as Montreal, extreme cold spells are linked with higher heating energy demand (Quayle & Diaz, 1980; Valor, Meneu, & Caselles, 2001; Zhao & Magoulès, 2012). As a result, magnitudes of extreme temperatures as well as durations of hot and cold days in a given year can provide proxies for magnitude and duration of high energy and/or water demands.

Table 2
Description of the 21 IPCC-CMIP5 climate models included in the NEX-GDDP downscaled climate scenarios. All these models are downscaled into a unique 0.25° × 0.25° grid resolution.

Model's name	Institution	Latitude resolution (°)	Longitude resolution (°)
ACCESS1-0	CSIRO (Commonwealth Scientific and Industrial Research Organisation, Australia), and BOM (Bureau of Meteorology, Australia)	1.25	1.875
CSIRO-MK3-6-0	Commonwealth Scientific and Industrial Research Organisation in collaboration with the Queensland Climate Change Centre of Excellence	1.8653	1.875
MIROC-ESM	Japan Agency for Marine-Earth Science and Technology, Atmosphere and Ocean Research Institute (The University of Tokyo), and National Institute for Environmental Studies	2.7906	2.8125
BCC-CSM1-1	Beijing Climate Center, China Meteorological Administration	2.7906	2.8125
GFDL-CM3	NOAA's Geophysical Fluid Dynamics Laboratory	2	2.5
MIROC-ESM-CHEM	Japan Agency for Marine-Earth Science and Technology, Atmosphere and Ocean Research Institute (The University of Tokyo), and National Institute for Environmental Studies	2.7906	2.8125
BNU-ESM	College of Global Change and Earth System Science, Beijing Normal University	2.7906	2.8125
GFDL-ESM2G	NOAA's Geophysical Fluid Dynamics Laboratory	2.0225	2
MIROC5	Japan Agency for Marine-Earth Science and Technology, Atmosphere and Ocean Research Institute (The University of Tokyo), and National Institute for Environmental Studies	1.4008	1.40625
CanESM2	Canadian Centre for Climate Modelling and Analysis	2.7906	2.8125
GFDL-ESM2M	NOAA's Geophysical Fluid Dynamics Laboratory	2.0225	2.5
MPI-ESM-LR	Max Planck Institute for Meteorology (MPI-M)	1.8653	1.875
CCSM4	National Center for Atmospheric Research	0.9424	1.25
INMCM4	Institute for Numerical Mathematics, Moscow, Russia	1.5	2
MPI-ESM-MR	Max Planck Institute for Meteorology (MPI-M)	1.8653	1.875
CESM1-BGC	National Science Foundation, Department of Energy, National Center for Atmospheric Research	0.9424	1.25
IPSL-CM5A-LR	Institut Pierre-Simon Laplace	1.8947	3.75
MRI-CGCM3	Meteorological Research Institute	1.12148	1.125
CNRM-CM5	Centre National de Recherches Météorologiques/Centre Européen de Recherche et Formation Avancées en Calcul Scientifique	1.4008	1.40625
IPSL-CM5A-MR	Institut Pierre-Simon Laplace	1.2676	2.5
NorESM1-M	Norwegian Climate Centre	1.8947	2.5

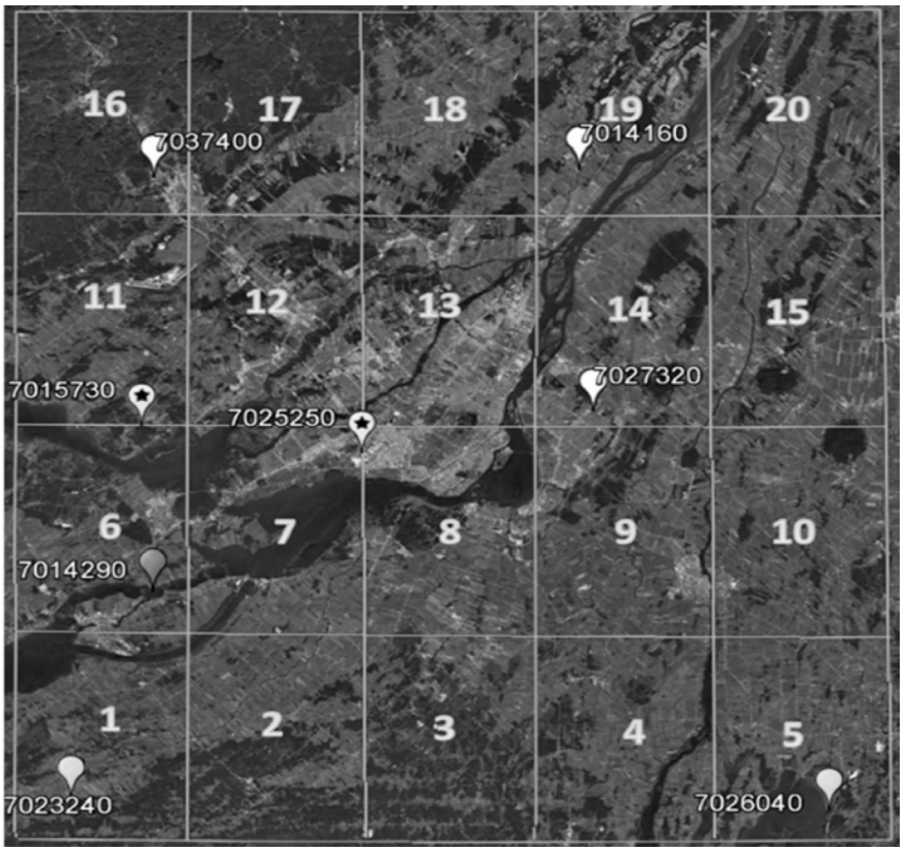

Fig. 1. The considered box representing the Greater Montreal and the surrounding regions, overlaid by 20 NEX-GDDP grids and 8 climate stations. The satellite image of Montreal was obtained from the Google Earth®.

Table 3
Nine annual hydroclimate variables relevant to water and energy security in the Greater Montreal area.

Annual variable	Unit	Relevance
Average of minimum daily temperature	°C	Expected range of annually-averaged daily water and energy demand
Average of maximum daily temperature	°C	Expected range of annually-averaged daily water and energy demand
Average of daily precipitation	mm	Expected annually-averaged daily local water availability
Extreme of daily maximum temperature	°C	Annual maximum water and cooling energy demands
Maximum daily precipitation	mm	Urban flooding
Extreme of daily minimum temperature	°C	Annual maximum heating energy demand
# of days with maximum temperature below 0°	–	Form of precipitation and hydrologic response (snow accumulation vs. runoff)
# of days with minimum temperature below −20°	–	Duration of high heating energy demand in winter seasons
# of days with maximum temperature above 30°	–	Duration of high water and cooling energy demands in summer seasons

4.2. Assessing the reliability of the downscaled climate product

During the retrospective period of 1950–2005, the nine hydroclimate variables introduced above can be calculated using the observed and twenty one downscaled daily climate simulations. While the observed ensemble includes annual time series obtained from 8 climate stations, each downscaled ensemble is based on the simulations of one climate model downscaled over 20 grids (see Fig. 1). Although local observations and gridded downscaled climate cannot be directly compared at a particular year and/or grid scale, the range of long-term spatiotemporal variability over the whole box region can be compared between the observed and downscaled ensembles. At this juncture, it is expected that downscaled ensembles, at least collectively, be able to represent the range obtained through gauged observations. To characterize the climate variability, we considered two key descriptive statistics, namely long-term mean and monotonic change. Monotonic change can describe the existence of trend in data and can be quantified using the Sen's slope estimate (Burns, Klaus, & McHale, 2007; Gocic & Trajkovic, 2013; Klaus, Chun, & Stumpp, 2015; Winslow, Read, Hansen, & Hanson, 2015; see Drápela & Drápelová, 2011 for complete formulation). To account for long-term climate, we considered varying 30-year time periods in both observed and downscaled ensembles. Thirty-year time periods have been widely used as the common time horizon for climate change impact assessment and/or to account for hydroclimate regime shift (e.g., Fleming & Sauchyn, 2013; Jones, Osborn, & Briffa, 2001; Webster, Holland, Curry, & Chang, 2005). To systematically account for temporal change in long-term statistics, we considered a moving window with the size of 30-year and slid it over each member within observed and downscaled ensembles year-by-year. Within each window, we calculated the long-term mean and the Sen's slope based on the 30-year time series framed within the window. By moving the window over the time series, the temporal evolution (first order temporal change) in long-term statistics can be quantified for a given hydroclimate variable, during the period spanning from 1950 to 2005 – see Nazemi, Wheater, Chun, Bonsal, and Mekonnen (2017) for more details on the moving window methodology. As an example, Fig. 2 shows how this approach can provide a notion for evolution in the 30-year expected mean and Sen's slope for

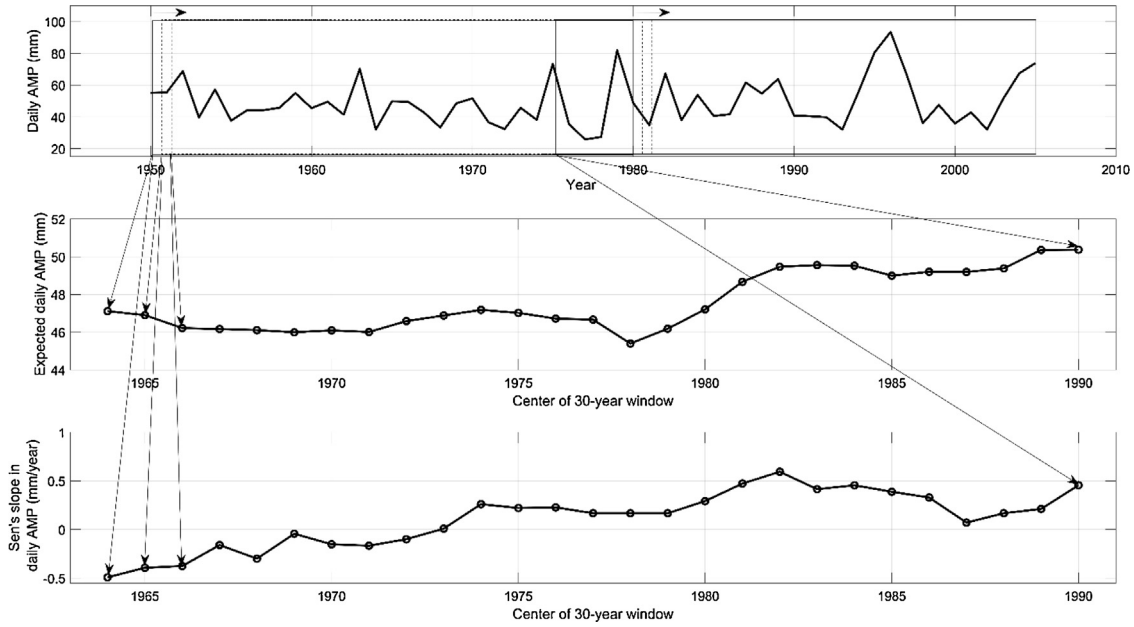

Fig. 2. Analyzing the evolution in expected long-term mean and Sen's slope in daily Annual Maximum Precipitation (AMP) using a 30-year moving window. First row shows the time series of the daily AMP in Montreal's International Airport (ID: 7025250). Second and third rows represent the mean and tend captured by a 30-year window moving year-by-year over the whole annual time series.

AMPs at Montreal's International Airport. The moving window methodology can be simply extended into a multi-member ensemble by repeating the procedure for all ensemble members. Accordingly, the temporal evolution in spatial variability (i.e. the range of 30-year statistics obtained in each window by all ensemble members) can provide a notion of spatiotemporal variability within the region during the study period.

4.3. Quantifying spatial variability and local uncertainty

As discussed above, the spatial variability in a hydroclimate variable can be intuitively represented by the ensemble's range. Accordingly, the risk of exceeding a particular value within this range can be quantified using a probability distribution that characterizes the empirical ratio of ensemble members in which the considered quantile is exceeded. Assuming that ensemble members contribute equally to the total information available on the spatial variability in the whole region, the empirical distribution can be further translated to the proportion of the total area (i.e. 20 grids in this study), in which a given value within the ensemble range is exceeded. While this assumption is wholly liable for gridded downscaled simulations, it can have some limitation in the case of observed ensembles as climate stations are not covering the total area equally. To avoid this problem, we spatially interpolated the climate observations into the 20 common grids for which the downscaled data are available. In brief, we transferred the information from climate stations to grid centers in which the stations are located. The information in ungauged grid centers are then reconstructed using gauged information and the Inverse Distance Weighting method (IDW; see Babak & Deutsch, 2009; Zimmerman, Pavlik, Ruggles, & Armstrong, 1999). By applying this spatial interpolation, the range of empirical observations remains unchanged; however the probability distribution would be corrected in a way that match the assumption made above.

To better articulate this, we demonstrate an example using observed and downscaled annual maximum daily precipitation data (hereafter daily Annual Maximum Precipitation; AMP) available for Montreal. Fig. 3a shows the ensemble of observed daily AMPs obtained from the 8 climate stations throughout the study region. Without losing generality, here we only consider exploring the spatial variability in one year (i.e. 1954), which is boxed in Fig. 3a. Using the IDW method, the observed values of AMP in year 1954 at the 8 gauge stations are transferred to the 20 grid centers to satisfy the assumption of equality in the information content of ensemble members (see Fig. 3b). The spatial variability with the box region can be then quantified using an empirical probability distribution (Fig. 3c), which shows the ratio of grids in which a certain AMP quantile is exceeded. As the area within grids is equal, this distribution can be directly translated into an empirical risk profile, quantifying the ratio of the total area in which a certain AMP quantile is exceeded (Fig. 3d). Here, we call such empirical distributions “Spatial Risk profiles” (SRPs), which quantify the empirical characteristics of spatial variability in the whole box region during a given time period. It is worthwhile to note that SRPs are grid-indifference. In other words, they only represent the percentage of grids in which a particular AMP quantile is exceeded but do not provide any information on which grids include such conditions.

As gauged observations are transferred into common grids as downscaled ensembles, the SRPs obtained from observed and downscaled product can be compared with one another. Fig. 3e compares the observed SRP with 21 simulated SRPs obtained from NEX-GDDP downscaled product. At this juncture, given a particular level of spatial risk (i.e. 20%, 80%, etc.), the risk of exceeding a particular AMP quantile in the light of 21 downscaled ensemble can be quantified using a secondary risk profile, termed here as “Local Risk Profile” (LRP). LRPs represent the percentage of models in which the considered AMP quantile at the given spatial risk level is exceeded. Fig. 3f shows the LRPs of 1954s AMP at 20% (dashed red profile) and 80% (solid red profile) exceedance levels in the light of 21 downscaled ensembles available through NEX-GDDP. Obviously at any given spatial risk, the observed ensemble is unique and therefore there is no local risk associated with the observed AMP – see black lines in Fig. 3f. SRPs and LRPs together can provide a formal tool to simultaneously account for spatial variability over the whole region and to represent the uncertainty in downscaled climate projections.

5. Results and discussion

5.1. Reliability of downscaled climate simulations

For each hydroclimate variables, the comparison between spatio-

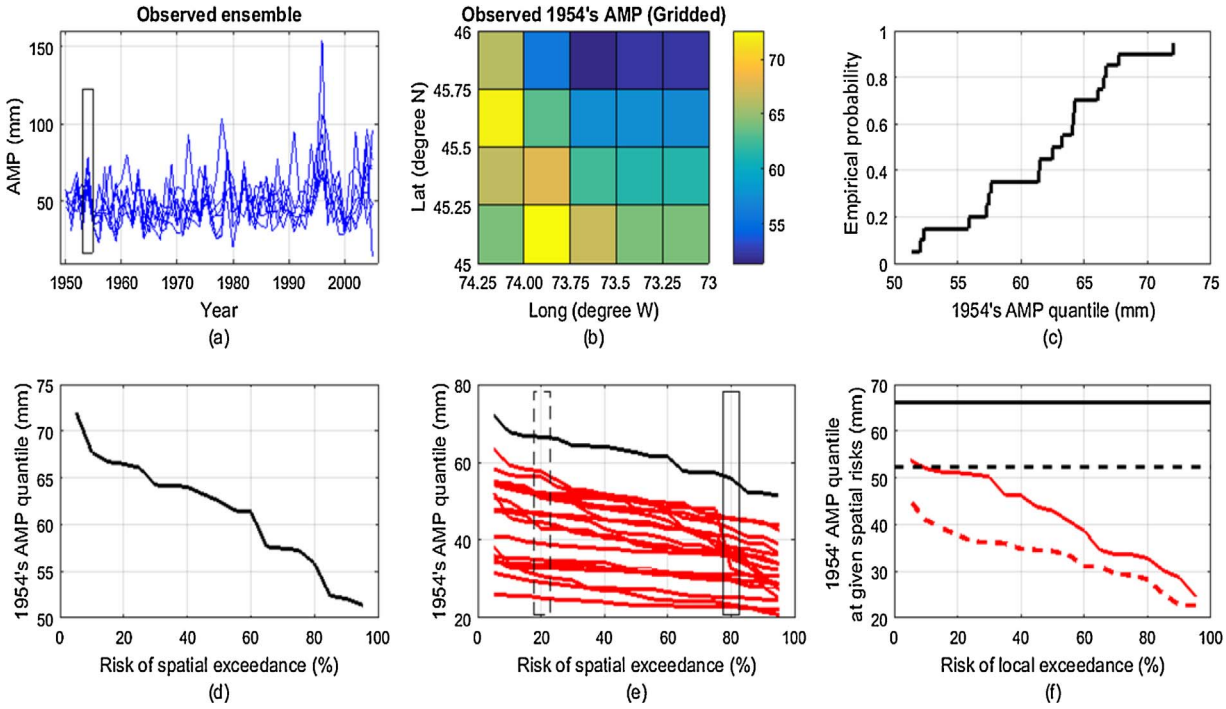

Fig. 3. Quantifying Spatial and Local Risk Profiles (SRPs and LRPs) using observed and downscaled Annual Maximum Precipitation (AMP) data in greater Montreal and surrounding regions. (a) The ensemble of gauged AMPs from 1950 to 2005; (b) the gridded observation in year 1954; (c) spatial variability in gridded observation in year 1954; (d) the 1954s SRP quantifying the ratio of the total area in which a certain AMP exceeds; (e) observed SRP (black) versus 21 downscaled SRPs for AMP in year 1954; (f) LRPs at 20% (dashed) and 80% (solid) spatial risks obtained from observed (black) and 21 downscaled ensembles (red). (For interpretation of the references to color in this figure legend, the reader is referred to the web version of the article.)

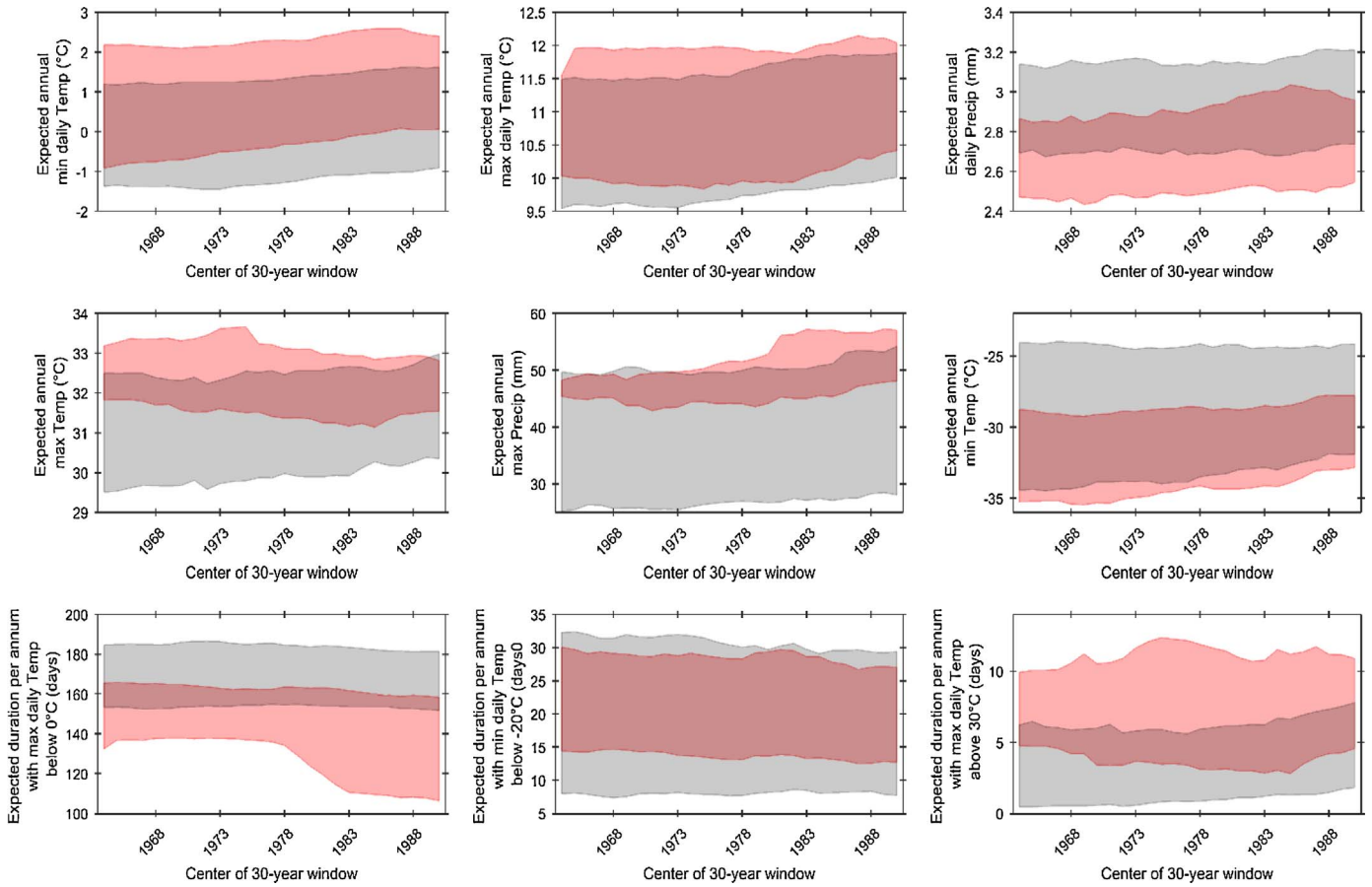

Fig. 4. Observed (pink) versus simulated (gray) evolutions in the 30-year means of the nine water security relevant hydroclimate variables in the Greater Montreal and surrounding neighboring regions. (For interpretation of the references to color in this figure legend, the reader is referred to the web version of the article.)

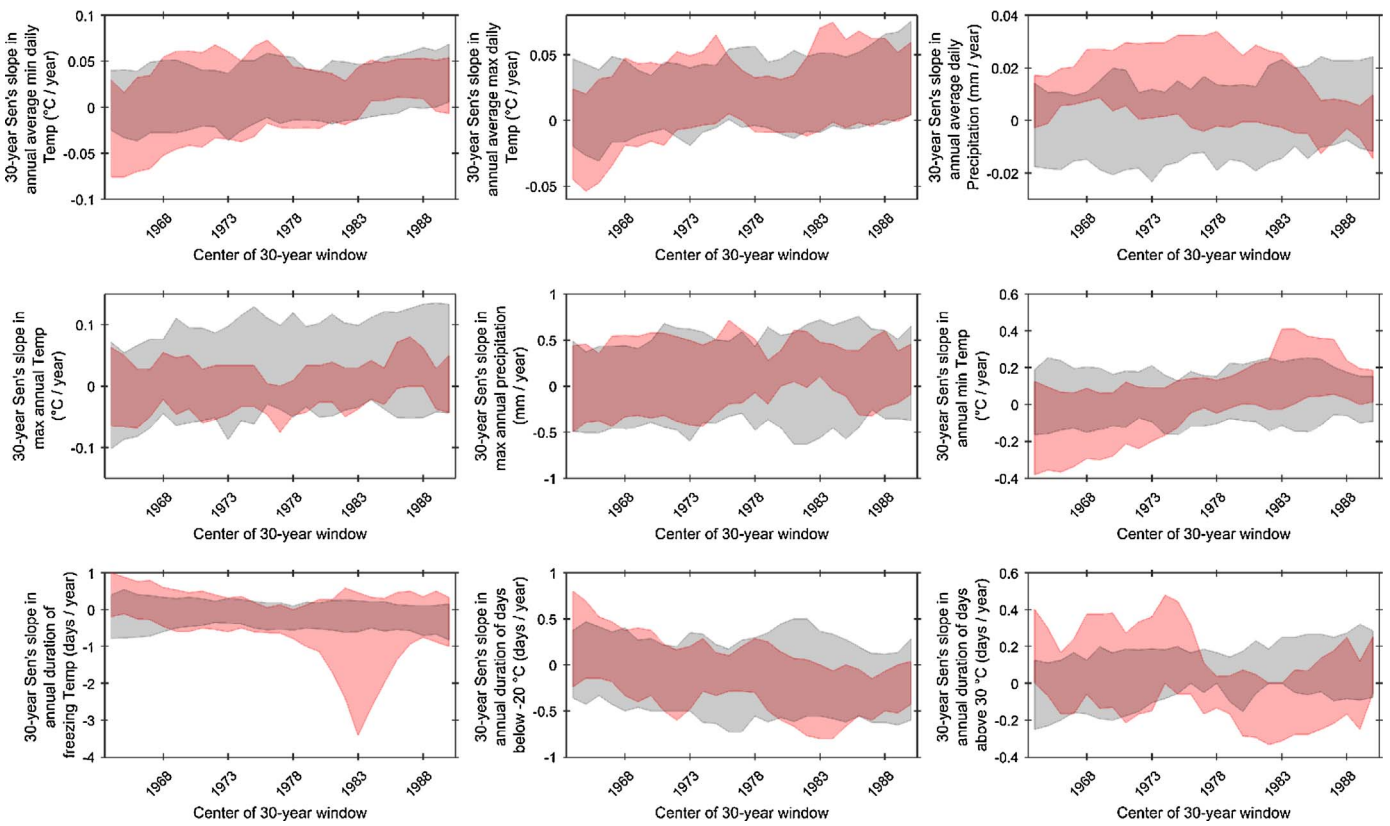

Fig. 5. Observed (pink) versus simulated (gray) evolutions in 30-year monotonic trends in nine water security relevant hydroclimate variables in the Greater Montreal and surrounding neighboring regions. The rate and direction of monotonic trend is characterized by the Sen's slope estimates. (For interpretation of the references to color in this figure legend, the reader is referred to the web version of the article.)

temporal evolutions in 30-year means and Sen's slopes between observed and downscaled ensembles can reveal how downscaled simulations can accurately represent the changes in observed climate over the Greater Montreal area. Figs. 4 and 5 compare the observed versus simulated spatiotemporal evolutions in expected long-term means and trends of the nine hydroclimate variables, respectively. The widths of envelopes show the spatial variability in the given descriptive statistics captured by the gridded climate observation ensemble (pink envelopes) and all 21 downscaled ensembles (gray envelopes). It should be noted that the gray envelopes collectively shows 420 downscaled realizations obtained from 21 models over 20 grids that cover the box region (see Fig. 1). Starting from long-term means, Fig. 4 vividly shows that in all considered variables, expected long-term means obtained from climate observations have a considerable spatial variability in the study region. This is quite important as the total area of the considered box region is still finer than one grid resolution of the majority of climate models used in the NEX-GDDP – see Table 2. As a result, downscaling is deemed important for capturing the in-grid variability of all hydroclimate variables. Nonetheless, there are considerable discrepancies between spatial variability captured by observed and downscaled ensembles, pointing that downscaled climate simulations, even collectively, are not able to fully capture the range of observed spatiotemporal variability. In brief, downscaled climate simulations consistently underestimate the range of long-term means for annual-average minimum and maximum daily temperatures. In contrast, downscaled climate simulations consistently overestimate the long-term mean of daily precipitation and therefore misrepresent the expected annual average of the local water availability. With respect to representing the expected long-term characteristics of annual temperature extremes, downscaled climate simulations underestimate and overestimate the magnitude of extreme warm and cold events, respectively, and therefore provide conservative representations of temperature extremes. Downscaled climate simulations also underestimate the observed ensemble of the expected maximum annual precipitation, particularly toward the end of the 20th century, when spatial variability in extreme precipitation has substantially increased in the region. Similarly, the expected annual numbers of days with below zero temperature and/or above 30 °C are considerably misrepresented by the downscaled climate simulations.

By looking at the observed evolutions in monotonic trends during the historical period shown in Fig. 5, considerable spatial variability can be also observed in the direction and the rate of change in all hydroclimate variables during the historical period. Similarly, comparing the evolution in the range of Sen's slopes between the observed and downscaled ensembles for each variable reveals how downscaled ensembles are collectively able to represent the rate and direction of change in all consecutive 30-year climate windows throughout the retrospective data period. Based on this analysis demonstrated in Fig. 5, it can be argued that downscaled climate simulations are not perfect in terms of representing the evolution of trend in some of the hydroclimate variables (e.g. annual extreme minimum temperature, number of days per annum with temperature above 30°); however, the observed range of spatiotemporal variability in monotonic trends are more-or-less captured by downscaled climate simulations for majority of considered hydroclimate variables.

Rather straight-forward analyses made above can shed light on the state of available downscaled climate simulation in the Greater Montreal and the surrounding regions: Although downscaled climate simulations cannot fully represent the range spatiotemporal variability in long-term means of considered annual hydroclimate variables, they can better capture the spatiotemporal variability of the monotonic trends during the historical period. As a result, looking into prospective downscaled climate projections can provide useful insights about the direction and rate of future changes in hydroclimate variables compared to the past.

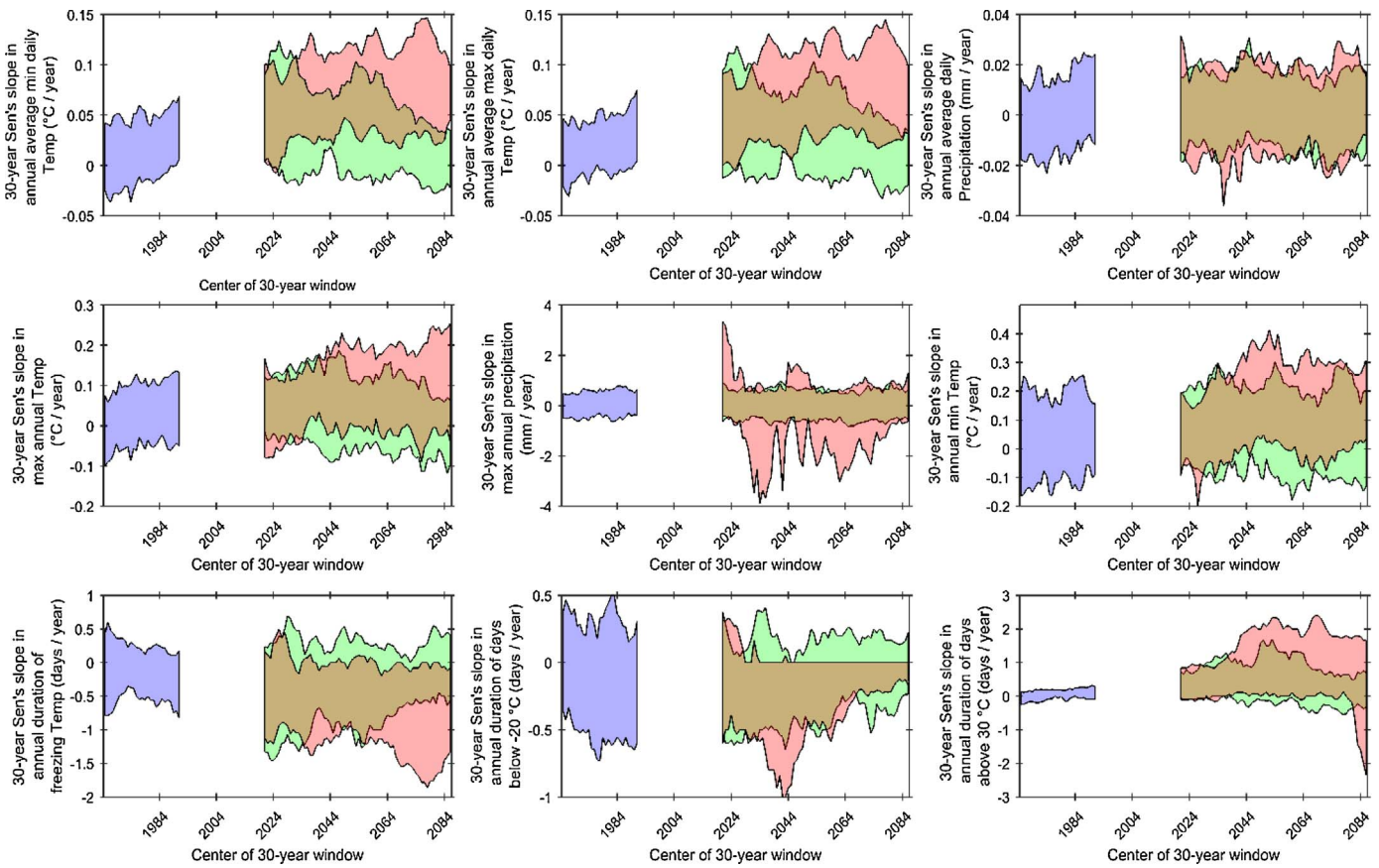

Fig. 6. Retrospective (blue) versus prospective evolutions in 30-year monotonic trends related to the nine water security relevant hydroclimate variables in the Greater Montreal and surrounding regions. The rate and direction of monotonic trend is characterized by the Sen's slope estimates. The future ensembles of trends are obtained for RCP 4.5 (green) and RCP 8.5 (pink). Brown envelopes represent overlap between RCP 4.5 and RCP 8.5 projections. (For interpretation of the references to color in this figure legend, the reader is referred to the web version of the article.)

Fig. 6 compares the spatiotemporal evolutions of 30-year trends between retrospective (1950–2005; blue envelope) and prospective downscaled simulations that are obtained by considering RCPs 4.5 (green envelope) and 8.5 (pink envelope) during 2006–2099. The brown envelopes represent overlap between RCP 4.5 and RCP 8.5 projections. The prospective evolutions in spatiotemporal variability of monotonic trends have been obtained similar to retrospective periods, using a moving window with the length of 30-year. This comparison can provide some critical information about the evolution of spatiotemporal changes in monotonic trends throughout the likely future climates. Most importantly, the spatial variability in the hydroclimate variables generally increases under future conditions. Having said that, the future evolutions of monotonic trends largely depend on the particular climate model and/or concentration pathway, with which the prospective ensemble is conditioned. As a result, substantial uncertainty is involved in the future projections, due to the uncertainty in the choice of climate models and/or the ambiguity introduced by characterizing the future concentration of the greenhouse gases.

5.2. Implications on urban management

Increased spatial variability in hydroclimate variables, in conjunction with uncertainty in future projections can introduce a range of complications for provision of effective urban management. Below, we try to demonstrate some of these obstacles using an example related to urban infrastructure design.

Precipitation extremes are critical to the design and operation of the storm water management systems in every city, including the Greater Montreal. In the engineering literature, the precipitation extremes are known as “design storms” and are often represented by intensity–duration–frequency curves (see e.g., Adams & Howard, 1986; Sivapalan & Blöschl, 1998). One major question for urban water managers is whether the current design storms are going to be altered as a result of the climate change (see e.g. Adamowski, Adamowski, & Bougadis, 2010; Madsen, Arnbjerg-Nielsen, & Mikkelsen, 2009); and if so, what kind of vulnerabilities are associated with urban infrastructures. Fig. 7 shows the estimated quantiles for 100-year daily precipitation extremes in the Greater Montreal and the surrounding regions during the recent past (i.e. 1971–2000; top left panel), as well as short-range (2010–2039; top right panel), mid-range (2040–2069; bottom left panel) and long-range (2070–2099; bottom right panel) futures. Future extreme quantiles are obtained based on prospective simulations under RCPs 4.5 and 8.5. We considered the 100-year return period as it has direct relevance to the design of key urban infrastructures for storm water management. For each time horizon, the 100-year daily rainfall extremes are estimated by fitting the Generalized Extreme Value Distribution (GEV; see Hosking, Wallis, & Wood, 1985; Martins & Stedinger, 2000; Morrison & Smith, 2002) to the observed and/or simulated AMPs (see Hassanzadeh, Nazemi, & Elshorbagy, 2014; Nazemi, Alam, & Elshorbagy, 2014; Nazemi, Elshorbagy, & Pingale, 2011). During the historical period, spatial variability in the 100-year rainfall is formally represented by SRPs obtained by observed (black line) and downscaled ensembles (colored envelopes). For downscaled SRPs, the width of the ensemble shows the uncertainty in the SRP due to differences in the climate models and/or RCPs.

Some crucial observations can be obtained from Fig. 7. Firstly, the solid black lines reveal that the historical 100-year daily design storm has been subject to significant spatial variability, changing from 75 mm to more than 150 mm in the Greater Montreal during the historical 1971–2000 baseline. This means that there is an immediate uncertainty associated with any single estimation of 100-year design storm for the

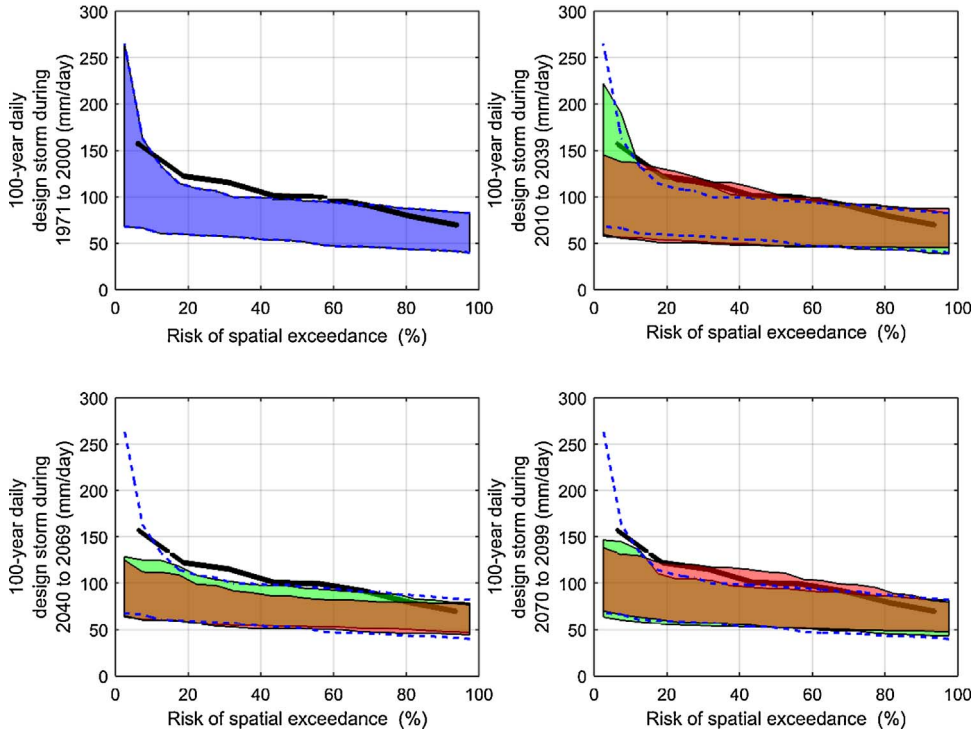

Fig. 7. Spatial Risk Profiles (SRPs) for 100-year daily rainfall extremes under the recent past (2071–2000; top left panel), short-range (2010–2039; top right panel), mid-range (2040–2069; bottom left panel) and long-range (2070–2099; bottom right panel) futures. Solid black lines show the SRP based on the observed climate. Envelopes represent the uncertainty in downscaled SRPs during historical (blue) and future periods, mapped under RCPs 4.5 (green) and 8.5 (pink) respectively. Brown envelopes represent the overlap between RCPs 4.5 and 8.5. The dashed blue lines show the lower and upper bounds of downscaled ensemble estimations during the historical period. (For interpretation of the references to color in this figure legend, the reader is referred to the web version of the article.)

whole region. On one hand, choosing smaller design storms for the entire region can result in underestimation of the rainfall extremes over a large area, which can increase the chance of urban flooding in the region. On the other hand, selecting higher design storms results in over-designing the storm water management system in many areas, which is associated with substantial increase in construction and operational costs. The spatial variability in design storms (and other hydroclimate variables) should be therefore recognized by urban water managers. Handling this heterogeneity would logically require moving toward more locally-relevant solutions rather than city-wide design criteria, for which the details of urbanization as well as socio-economic developments play an important role (see also Chang & Bonnette, 2016).

Secondly, the model-based ensemble estimation of the SRP during the historical period has considerable discrepancy compared to the one obtained from climate observations. The nature of this error in downscaled SRPs is rather complex as the magnitude of the error changes at different spatial exceedance levels. This requires further “localization” of downscaled climate simulation to adjust them in a way that the mean ensemble provides an unbiased representation of the gridded historical climate. Such localization can be done using rather simple (see Christensen, Boberg, Christensen, & Lucas-Picher, 2008; Teutschbein & Seibert, 2012), continuous (e.g., Chun, Wheater, Nazemi, & Khaliq, 2013) and quantile-based downscaling approaches (e.g., Hassanzadeh et al., 2014; Srivastav, Schardong, & Simonovic, 2014). Accordingly, future projections can be updated to provide a revised notion of change in the SRPs, in the light of available climate projections. Nonetheless, it should be noted that even after further localization, there would be still considerable uncertainty in assigning a particular design storm at each grid within the region. This is due to the fact that the choice of climate model and/or concentration pathway can drastically alter the estimated extreme rainfall values. One way to handle this would be relying on the ensemble mean (Graham, Andréasson, & Carlsson, 2007; Meehl et al., 2007). More sophisticated approach would be to give weights to downscaled climate simulations based on how well they can capture the observed design storm during the historical period (see e.g., Giorgi & Mearns, 2003; Räisänen, Ruokolainen, & Ylhäisi, 2010; Tebaldi, Smith, Nychka, & Mearns, 2005). The future design storm can be then estimated as the weighted average of available ensemble members. Both approaches are subject to large uncertainty as they are based on assumptions that the error structure in the ensemble members remains unchanged between retrospective and prospective simulations. Alternatively, the uncertainty in the design storm at each point can be described using a formal LRP, which quantifies the chance of exceeding a particular design storm at the local scale, in the light of the localized climate projections, obtained from various climate models and/or concentration pathways. Such LRPs can then assist water managers to choose a particular design storm from the available ensemble members, in a way that it can make an optimal trade-off between risk of flooding at the point of interest and budgetary constraints.

6. Summary and concluding remarks

Supporting human life and socio-economic activities in urban regions require continuous water supply as well as high resilience against adverse effects of floods and droughts. Growing population and socio-economic activities on one hand, and emerging effect of climate change on the other hand, can majorly threaten water security in cities around the world. Climate change, in particular, directly affects water demand, water availability and hydroclimate extremes to which human activities in urban regions are vulnerable. The effect of climate change on urban water security therefore should be urgently assessed with the greater goal of providing the scientific knowledge required for adapting operational policies and/or governance options. The most essential requirement for this effort is the availability of high-quality data support, with which the effect of climate change can be expressed at the fine spatial resolution. The advent of various downscaling techniques has recently addressed the issue of scale mismatch associated with global climate models; however, it is still unclear whether the down-

scaled gridded climate products can adequately inform impact models and be readily used for assessing the climate impacts at the scale relevant to individual cities. In this paper, we have addressed how retrospective downscaled climate simulations are able to reproduce observed spatiotemporal variability in long-term mean and trend, related to a set of annual hydroclimate variables that have relevance to water and energy security in Montreal, Canada. Using the high-quality climate observations in 8 locations throughout the Greater Montreal, we have shown that even in the sub-grid resolution of majority of IPCC-CMIP5 models, substantial spatial variability in all considered hydroclimate variables can be observed. Using the moving window methodology, we have shown that spatial variability in 30-year mean and trend for the considered hydroclimate variables is changing over time, with the possibility for more pronounced change under climate change scenarios. Having said that, prospective downscaled climate simulations should be treated with caution for two key reasons. Most importantly, although retrospective downscaled climate simulations can collectively capture the rate and direction of the long-term trends in considered hydroclimate variables, they have substantial discrepancies in reproducing the long-term means during the historical period. In additions, there is an inherent uncertainty in future projections, due to uncertainties in the future concentration of greenhouse gasses.

The above issues pose major challenges to urban management. We tried to demonstrate some of these challenges using a real-world design problem, involving the identification of 100-year daily extreme rainfall in the city of Montreal. We have shown that due to the considerable spatial variability, estimating one design storm for the entire city will not be possible, which means that the urban management should move more toward local rather than city-wide solutions. In addition, there is a substantial error in reproducing the observed SRPs, which necessitates further localization, using bias correction and/or downscaling algorithms. We also suggested LRPs to properly communicate the uncertainty in the SPRs as the result of different climate models forced under a range of RCPs. This can provide a basis for improved decision at local scales.

It should be noted that while suggested SRPs and LRPs can provide formal tools to account for spatial variability and local uncertainty in downscaled hydroclimate variables, they become outdated as soon as new climate projections become available. This poses major complexities for decision making as they would be subject to change during the period of infrastructure operations. As a result, it has been suggested that future climate projections should be taken only as guidelines (Beven, 2011; Pielke & Wilby, 2012). Even if a perfect climate model is available, the future projections are wholly subject to particular concentration pathways that might be significantly different from real-world concentration of greenhouse gases. This inherent uncertainty can further propagate into assessing the future vulnerabilities and translate into major sources of uncertainty in addressing water security threats in cities around the world. We suggest, therefore, that urban water managers should be conscious about the limitations in the current downscaled climate projections and move toward more holistic frameworks that can help identifying potential sources of vulnerability under a wide range of possible climate futures, until improved climate modeling capability become available. "Bottom-up" schemes based on various "stress-tests" are recently emerging that can be effectively used for this purpose (see e.g., Brown & Wilby, 2012). Such approaches require a range of change in hydroclimate variables that can be obtained with or without considering downscaled projections. Accordingly, the purpose of the assessment is to map the response of the system to the considered range of change, with a greater goal of identifying critical thresholds, under which the system becomes vulnerable. Adaptation strategies can be then tested to see how the identified vulnerabilities can be reduced given operational restrictions. Such approaches have been successfully applied in the context of regional water resource management (see e.g. Hassanzadeh, Elshorbagy, Wheater, & Gober, 2016; Hassanzadeh, Elshorbagy, Wheater, Gober, & Nazemi, 2015; Nazemi, Wheater, Chun, & Elshorbagy, 2013) and can be readily transferred to address the potential vulnerabilities to urban water security as a result of changing climate. It should be noted that "bottom-up" approaches are also limited (see e.g., Nazemi & Wheater, 2014); as a result, in a broader adaptation context the results of "top-down" and "bottom-up" assessments should be merged within a hybrid assessment framework to provide a set of decision-centric and locally-relevant solutions to urban water security threats as a result of changing climate (see Armstrong, Wilby, & Nicholls, 2015; Chang & Bonnette, 2016).

Climate change already is, and will continue to be, one of the major environmental threats to cities around the world. We hope that by showcasing the observed spatiotemporal variability and state of climate projections in Montreal, we could be able to shed light on some of the challenges in assessing the impacts of climate change on urban water security and future engineering designs globally. We encourage accounting for current limitations in climate modeling technology, which requires efforts toward building enhanced tools and methodologies that can inform urban planner and decision makers about the potential water security threats as a result of the changing climate.

Acknowledgments

Downscaled climate scenarios used were from the NASA Earth Exchange Global Daily Downscaled Projections (NEX-GDDP) dataset, prepared by the Climate Analytics Group and NASA Ames Research Center using the NASA Earth Exchange, and distributed by the NASA Center for Climate Simulation (NCCS) – see https://cds.nccs.nasa.gov/nex-gddp/. Historical climate in Canada can be accessed through Environment and Climate Change Canada's Historical Climate Archive at http://climate.weather.gc.ca/historical_data/search_historic_data_e.html. We are grateful to the extremely constructive comments provided by three anonymous reviewers, which helped us to significantly improve the quality of our initial submission. Financial support for this study is provided by the Concordia University through Startup and Strategic Hire Funds as well as Graduate Students' Scholarship Program.

References

Adamowski, J., Adamowski, K., & Bougadis, J. (2010). Influence of trend on short duration design storms. *Water Resources Management*, *24*(3), 401–413.

Adams, B. J., & Howard, C. D. (1986). Design storm pathology. *Canadian Water Resources Journal*, *11*(3), 49–55.

Armstrong, J., Wilby, R., & Nicholls, R. (2015). Climate change adaptation frameworks: An evaluation of plans for coastal Suffolk, UK. *Natural Hazards and Earth System Science*, *15*, 2511–2524.

Babak, O., & Deutsch, C. V. (2009). Statistical approach to inverse distance interpolation. *Stochastic Environmental Research and Risk Assessment*, *23*(5), 543–553.

Barroca, B., Bernardara, P., Mouchel, J. M., & Hubert, G. (2006). Indicators for identification of urban flooding vulnerability. *Natural Hazards and Earth System Science*, *6*(4), 553–561.

Beven, K. (2011). I believe in climate change but how precautionary do we need to be in planning for the future? *Hydrological Processes*, *25*(9), 1517–1520. http://dx.doi.org/10.1002/hyp7939.

Bougadis, J., Adamowski, K., & Diduch, R. (2005). Short-term municipal water demand forecasting. *Hydrological Processes*, *19*(1), 137–148.

Breyer, B., Chang, H., & Parandvash, G. H. (2012). Land-use, temperature, and single-family residential water use patterns in Portland, Oregon and Phoenix, Arizona. *Applied Geography*, *35*(1), 142–151.

Brown, C., & Wilby, R. L. (2012). An alternate approach to assessing climate risks. *Eos, Transactions of American Geophysical Union*, *93*(41), 401. http://dx.doi.org/10.1029/2012EO410001.

Brown, W. M., & Rispoli, L. (2014). *Metropolitan gross domestic product: Experimental estimates, 2001 to 2009*. Available at: http://www.statcan.gc.ca/pub/11-626-x/11-626-x2014042-eng.pdf (retrieved).

Burns, D. A., Klaus, J., & McHale, M. R. (2007). Recent climate trends and implications for water resources in the Catskill Mountain region, New York, USA. *Journal of Hydrology*, *336*(1), 155–170.

CBC (2011). *Electricity in Quebec*. http://www.cbc.ca/news/canada/electricity-in-quebec-1.1094675.

Chang, H., & Bonnette, M. R. (2016). Climate change and water-related ecosystem services: Impacts of drought in California, USA. *Ecosystem Health and Sustainability*, *2*(12).

Chang, H., Praskievicz, S., & Parandvash, H. (2014). Sensitivity of urban water

consumption to weather and climate variability at multiple temporal scales: The case of Portland, Oregon. *International Journal of Geospatial and Environmental Research*, *1*(1), 7.
Chen, Y., Zhou, H., Zhang, H., Du, G., & Zhou, J. (2015). Urban flood risk warning under rapid urbanization. *Environmental Research*, *139*, 3–10.
Christensen, J. H., Boberg, F., Christensen, O. B., & Lucas-Picher, P. (2008). On the need for bias correction of regional climate change projections of temperature and precipitation. *Geophysical Research Letters*, *35*(20).
Chun, K. P., Wheater, H. S., Nazemi, A., & Khaliq, M. N. (2013). Precipitation downscaling in Canadian Prairie Provinces using the LARS-WG and GLM approaches. *Canadian Water Resources Journal*, *38*(4), 311–332.
Colombo, A. F., Etkin, D., & Karney, B. W. (1999). Climate variability and the frequency of extreme temperature events for nine sites across Canada: Implications for power usage. *Journal of Climate*, *12*(8), 2490–2502.
Crutzen, P. J. (2006). *The "anthropocene". Earth system science in the anthropocene*, . Berlin, Heidelberg: Springer, 13–18.
Cutter, S. L. (1996). Vulnerability to environmental hazards. *Progress in Human Geography*, *20*(4), 529–539.
Daniel, M., Lemonsu, A., & Viguié, V. (2016). Role of watering practices in large-scale urban planning strategies to face the heat-wave risk in future climate. *Urban Climate*. http://dx.doi.org/10.1016/j.uclim.2016.11.001.
Drápela, K., & Drápelová, I. (2011). Application of Mann-Kendall test and the Sen's slope estimates for trend detection in deposition data from Bílý Kříž (Beskydy Mts., the Czech Republic) 1997–2010. *Beskydy*, *4*(2), 133–146.
Environment Canada (1987). *The climate of Montreal (No. 4). Report prepared by Environment Canada, Atmospheric Environment Service, & Canadian Climate Program* Ottawa, Canada: Available from Canadian Government Pub. Centre, Supply and Services Canada.
Fleming, S. W., & Sauchyn, D. J. (2013). Availability, volatility, stability, and teleconnectivity changes in prairie water supply from Canadian Rocky Mountain sources over the last millennium. *Water Resources Research*, *49*(1), 64–74. http://dx.doi.org/10.1029/2012WR012831.
Franczyk, J., & Chang, H. (2009). Spatial analysis of water use in Oregon, USA, 1985–2005. *Water Resources Management*, *23*(4), 755–774.
Ghiassi, M., Zimbra, D. K., & Saidane, H. (2008). Urban water demand forecasting with a dynamic artificial neural network model. *Journal of Water Resources Planning and Management*, *134*(2), 138–146.
Giorgi, F., & Mearns, L. O. (2003). Probability of regional climate change based on the Reliability Ensemble Averaging (REA) method. *Geophysical Research Letters*, *30*(12).
Gleick, P. H. (2003). Water use. *Annual Review of Environment and Resources*, *28*(1), 275–314.
Gocic, M., & Trajkovic, S. (2013). Analysis of changes in meteorological variables using Mann-Kendall and Sen's slope estimator statistical tests in Serbia. *Global and Planetary Change*, *100*, 172–182.
Graham, L. P., Andréasson, J., & Carlsson, B. (2007). Assessing climate change impacts on hydrology from an ensemble of regional climate models, model scales and linking methods – A case study on the Lule River basin. *Climatic Change*, *81*(1), 293–307.
Guhathakurta, S., & Gober, P. (2007). The impact of the Phoenix urban heat island on residential water use. *Journal of the American Planning Association*, *73*(3), 317–329.
Hallegatte, S., Green, C., Nicholls, R. J., & Corfee-Morlot, J. (2013). Future flood losses in major coastal cities. *Nature Climate Change*, *3*(9), 802–806.
Hanasaki, N., Fujimori, S., Yamamoto, T., Yoshikawa, S., Masaki, Y., Hijioka, Y., et al. (2013). A global water scarcity assessment under Shared Socio-economic Pathways – Part 1: Water use. *Hydrology and Earth System Sciences*, *17*(7), 2375–2391.
Harding, K. J., Snyder, P. K., & Liess, S. (2013). Use of dynamical downscaling to improve the simulation of Central US warm season precipitation in CMIP5 models. *Journal of Geophysical Research: Atmospheres*, *118*(22).
Hassanzadeh, E., Elshorbagy, A., Wheater, H., & Gober, P. (2016). A risk-based framework for water resource management under changing water availability, policy options, and irrigation expansion. *Advances in Water Resources*, *94*, 291–306.
Hassanzadeh, E., Elshorbagy, A., Wheater, H., Gober, P., & Nazemi, A. (2015). Integrating supply uncertainties from stochastic modeling into integrated water resource management: A case study of the Saskatchewan River Basin. *ASCE Journal of Water Resources Planning and Management*, *142*(2), 05015006.
Hassanzadeh, E., Nazemi, A., & Elshorbagy, A. (2014). Quantile-based downscaling of precipitation using genetic programming: Application to IDF curves in Saskatoon. *Journal of Hydrologic Engineering*, *19*(5), 943–955.
Hejazi, M., Edmonds, J., Chaturvedi, V., Davies, E., & Eom, J. (2013). Scenarios of global municipal water-use demand projections over the 21st century. *Hydrological Sciences Journal*, *58*(3), 519–538.
Hejazi, M., Edmonds, J., Clarke, L., Kyle, P., Davies, E., Chaturvedi, V., et al. (2014). Long-term global water projections using six socioeconomic scenarios in an integrated assessment modeling framework. *Technological Forecasting and Social Change*, *81*, 205–226.
Hollis, G. E. (1975). The effect of urbanization on floods of different recurrence interval. *Water Resources Research*, *11*(3), 431–435.
Hosking, J. R., Wallis, J. R., & Wood, E. F. (1985). Estimation of the generalized extreme-value distribution by the method of probability-weighted moments. *Technometrics*, *27*(3), 251–261.
House-Peters, L. A., & Chang, H. (2011). Urban water demand modeling: Review of concepts, methods, and organizing principles. *Water Resources Research*, *47*, W05401. http://dx.doi.org/10.1029/2010WR009624.
Huong, H. T. L., & Pathirana, A. (2013). Urbanization and climate change impacts on future urban flooding in Can Tho city, Vietnam. *Hydrology and Earth System Sciences*, *17*(1), 379–394.
Ibrahim, N., Sugar, L., Hoornweg, D., & Kennedy, C. (2012). Greenhouse gas emissions from cities: Comparison of international inventory frameworks. *Local Environment*, *17*(2), 223–241.
Iglesias, A., Garrote, L., Diz, A., Schlickenrieder, J., & Martin-Carrasco, F. (2011). Re-thinking water policy priorities in the Mediterranean region in view of climate change. *Environmental Science & Policy*, *14*(7), 744–757.
Intergovernmental Panel on Climate Change (2014). *Climate change 2014 – Impacts, adaptation and vulnerability: Regional aspects*. Cambridge University Press.
Jones, P. D., Osborn, T. J., & Briffa, K. R. (2001). The evolution of climate over the last millennium. *Science*, *292*(5517), 662–667.
Kenney, D. S., Goemans, C., Klein, R., Lowrey, J., & Reidy, K. (2008). Residential water demand management: Lessons from Aurora, Colorado1. *JAWRA Journal of the American Water Resources Association*, *44*, 192–207. http://dx.doi.org/10.1111/j.1752-1688.2007.00147.x.
Klaus, J., Chun, K. P., & Stumpp, C. (2015). Temporal trends in $\delta^{18}O$ composition of precipitation in Germany: Insights from time series modelling and trend analysis. *Hydrological Processes*, *29*, 2668–2680. http://dx.doi.org/10.1002/hyp10395.
Lewis, S. C. (2011). *Energy in the smart home. The connected home: The future of domestic life*, . London: Springer, 281–300.
Madsen, H., Arnbjerg-Nielsen, K., & Mikkelsen, P. S. (2009). Update of regional intensity–duration–frequency curves in Denmark: Tendency towards increased storm intensities. *Atmospheric Research*, *92*(3), 343–349.
Maidment, D. R., Miaou, S. P., & Crawford, M. M. (1985). Transfer function models of daily urban water use. *Water Resources Research*, *21*(4), 425–432.
Martins, E. S., & Stedinger, J. R. (2000). Generalized maximum-likelihood generalized extreme-value quantile estimators for hydrologic data. *Water Resources Research*, *36*(3), 737–744.
McDonald, R. I., Green, P., Balk, D., Fekete, B. M., Revenga, C., Todd, M., et al. (2011). Urban growth, climate change, and freshwater availability. *Proceedings of the National Academy of Sciences of the United States of America*, *108*(15), 6312–6317.
Mearns, L. O., Sain, S., Leung, L. R., Bukovsky, M. S., McGinnis, S., Biner, S., et al. (2013). Climate change projections of the North American regional climate change assessment program (NARCCAP). *Climatic Change*, *120*(4), 965–975.
Meehl, G. A., Covey, C., Delworth, T., Latif, M., McAvaney, B., Mitchell, J., et al. (2007). The WCRP CMIP3 multi-model dataset: A new era in climate change research. *Bulletin of the American Meteorological Society*, *88*, 1383–1394.
Meinshausen, M., Smith, S. J., Calvin, K., Daniel, J. S., Kainuma, M. L. T., Lamarque, J. F., et al. (2011). The RCP greenhouse gas concentrations and their extensions from 1765 to 2300. *Climatic Change*, *109*(1–2), 213–241.
Mirhosseini, G., Srivastava, P., & Stefanova, L. (2013). The impact of climate change on rainfall Intensity–Duration–Frequency (IDF) curves in Alabama. *Regional Environmental Change*, *13*(1), 25–33.
Mokrech, M., Kebede, A. S., Nicholls, R. J., Wimmer, F., & Feyen, L. (2015). An integrated approach for assessing flood impacts due to future climate and socio-economic conditions and the scope of adaptation in Europe. *Climatic Change*, *128*(3–4), 245–260.
Morrison, J. E., & Smith, J. A. (2002). Stochastic modeling of flood peaks using the generalized extreme value distribution. *Water Resources Research*, *38*(12).
Nazemi, A., Alam, M., & Elshorbagy, A. (2014). Uncertainties in future projections of extreme rainfall: The role of climate model, emission scenario and randomness. *Proceedings of the 11th international conference on hydroinformatics* Available at: http://academicworks.cuny.edu/cgi/viewcontent.cgi?article=1144&context=cc_conf_hic.
Nazemi, A., Elshorbagy, A., & Pingale, S. (2011). Uncertainties in the estimation of future annual extreme daily rainfall for the city of Saskatoon under climate change effects. *20th Canadian hydrotechnical conference*.
Nazemi, A., & Wheater, H. (2014). Assessing the vulnerability of water supply to changing streamflow conditions. *Eos, Transactions of American Geophysical Union*, *95*(32), 288.
Nazemi, A., & Wheater, H. S. (2015a). On inclusion of water resource management in Earth system models – Part 1: Problem definition and representation of water demand. *Hydrology and Earth System Sciences*, *19*(1), 33–61.
Nazemi, A., & Wheater, H. S. (2015b). On inclusion of water resource management in Earth system models – Part 2: Representation of water supply and allocation and opportunities for improved modeling. *Hydrology and Earth System Sciences*, *19*(1), 63–90.
Nazemi, A., Wheater, H. S., Chun, K. P., Bonsal, B., & Mekonnen, M. (2017). Forms and drivers of annual streamflow variability in the headwaters of Canadian Prairies during the 20th century. *Hydrological Processes*. http://dx.doi.org/10.1002/hyp.11036.
Nazemi, A., Wheater, H. S., Chun, K. P., & Elshorbagy, A. (2013). A stochastic reconstruction framework for analysis of water resource system vulnerability to climate-induced changes in river flow regime. *Water Resources Research*, *49*(1), 291–305.
Nkomo, S., & van der Zaag, P. (2004). Equitable water allocation in a heavily committed international catchment area: The case of the Komati Catchment. *Physics and Chemistry of the Earth, Parts A/B/C*, *29*(15), 1309–1317.
Parandvash, G. H., & Chang, H. (2016). Analysis of long-term climate change on per capita water demand in urban versus suburban areas in the Portland metropolitan area, USA. *Journal of Hydrology*, *538*, 574–586.
Parkinson, S. C., Johnson, N., Rao, N. D., Jones, B., van Vliet, M. T., Fricko, O., et al. (2016). Climate and human development impacts on municipal water demand: A spatially-explicit global modeling framework. *Environmental Modelling & Software*, *85*, 266–278.
Pielke, R. A., Sr., & Wilby, R. L. (2012). Regional climate downscaling: What's the point? *Eos, Transactions of American Geophysical Union*, *93*(5), 52. http://dx.doi.org/10.1029/2012EO050008.
Pomeroy, J. W., Stewart, R. E., & Whitfield, P. H. (2016). The 2013 flood event in the

South Saskatchewan and Elk River basins: Causes, assessment and damages. *Canadian Water Resources Journal/Revue canadienne des ressources hydriques*, *41*(1–2), 105–117.
Praskievicz, S., & Chang, H. (2009). Identifying the relationships between urban water consumption and weather variables in Seoul, Korea. *Physical Geography*, *30*(4), 324–337.
Quayle, R. G., & Diaz, H. F. (1980). Heating degree day data applied to residential heating energy consumption. *Journal of Applied Meteorology*, *19*(3), 241–246.
Räisänen, J., Ruokolainen, L., & Ylhäisi, J. (2010). Weighting of model results for improving best estimates of climate change. *Climate Dynamics*, *35*(2–3), 407–422.
Riga, A. (2016, January 12). Why do Montreal water mains burst so often. *Montreal Gazette*.
Rodríguez, R., Navarro, X., Casas, M. C., Ribalaygua, J., Russo, B., Pouget, L., et al. (2014). Influence of climate change on IDF curves for the metropolitan area of Barcelona (Spain). *International Journal of Climatology*, *34*(3), 643–654.
Schreider, S. Y., Smith, D. I., & Jakeman, A. J. (2000). Climate change impacts on urban flooding. *Climatic Change*, *47*(1), 91–115.
Seto, K. C., Güneralp, B., & Hutyra, L. R. (2012). Global forecasts of urban expansion to 2030 and direct impacts on biodiversity and carbon pools. *Proceedings of the National Academy of Sciences of the United States of America*, *109*(40), 16083–16088.
Seto, K. C., Sánchez-Rodríguez, R., & Fragkias, M. (2010). The new geography of contemporary urbanization and the environment. *Annual Review of Environment and Resources*, *35*, 167–194.
Sheffield, J., Goteti, G., & Wood, E. F. (2006). Development of a 50-yr high-resolution global dataset of meteorological forcings for land surface modeling. *Journal of Climate*, *19*(13), 3088–3111.
Simonovic, S. P., Schardong, A., & Sandink, D. (2016). Mapping extreme rainfall statistics for Canada under climate change using updated intensity–duration–frequency curves. *Journal of Water Resources Planning and Management*, 04016078.
Sivapalan, M., & Blöschl, G. (1998). Transformation of point rainfall to areal rainfall: Intensity–duration–frequency curves. *Journal of Hydrology*, *204*(1), 150–167.
Smith, D. I., & Handmer, J. W. (1984). Urban flooding in Australia: Policy development and implementation. *Disasters*, *8*(2), 105–117.
Srivastav, R. K., Schardong, A., & Simonovic, S. P. (2014). Equidistance quantile matching method for updating IDF curves under climate change. *Water Resources Management*, *28*(9), 2539–2562.
Statistics Canada (2012). *Population and dwelling counts, for population centres, 2011 and 2006 censuses*. Available at: http://www12.statcan.gc.ca/census-recensement/2011/dp-pd/hlt-fst/pd-pl/Table-Tableau.cfm?LANG=Eng&T=801&PR=0&RPP=9999&SR=1&S=3&O=D (retrieved).
Steffen, W., Crutzen, P. J., & McNeill, J. R. (2007). The Anthropocene: Are humans now overwhelming the great forces of nature. *AMBIO: A Journal of the Human Environment*, *36*(8), 614–621.
Steffen, W., Grinevald, J., Crutzen, P., & McNeill, J. (2011). The Anthropocene: Conceptual and historical perspectives. *Philosophical Transactions of the Royal Society of London A: Mathematical, Physical and Engineering Sciences*, *369*(1938), 842–867.
Steffen, W., Persson, Å., Deutsch, L., Zalasiewicz, J., Williams, M., Richardson, K., et al. (2011). The Anthropocene: From global change to planetary stewardship. *AMBIO: A Journal of the Human Environment*, *40*(7), 739–761.
Taylor, K. E., Stouffer, R. J., & Meehl, G. A. (2012). An overview of CMIP5 and the experiment design. *Bulletin of the American Meteorological Society*, *93*(4), 485.
Tebaldi, C., Smith, R. L., Nychka, D., & Mearns, L. O. (2005). Quantifying uncertainty in projections of regional climate change: A Bayesian approach to the analysis of multimodel ensembles. *Journal of Climate*, *18*(10), 1524–1540.
Teutschbein, C., & Seibert, J. (2012). Bias correction of regional climate model simulations for hydrological climate-change impact studies: Review and evaluation of different methods. *Journal of Hydrology*, *456*, 12–29.
Tewathia, N. (2014). Determinants of the household electricity consumption: A case study of Delhi. *International Journal of Energy Economics and Policy*, *4*(3), 337.
Thrasher, B., Maurer, E. P., McKellar, C., & Duffy, P. B. (2012). Technical note: Bias correcting climate model simulated daily temperature extremes with quantile mapping. *Hydrology and Earth System Sciences*, *16*(9).
Thrasher, B., Xiong, J., Wang, W., Melton, F., Michaelis, A., & Nemani, R. (2013). Downscaled climate projections suitable for resource management. *Eos, Transactions of American Geophysical Union*, *94*(37), 321–323.
Tian, D., Martinez, C. J., & Asefa, T. (2016). Improving short-term urban water demand forecasts with reforecast analog ensembles. *Journal of Water Resources Planning and Management*, *142*(6), 04016008.
Timm, O. E., Giambelluca, T. W., & Diaz, H. F. (2015). Statistical downscaling of rainfall changes in Hawai'i based on the CMIP5 global model projections. *Journal of Geophysical Research: Atmospheres*, *120*(1), 92–112.
Valor, E., Meneu, V., & Caselles, V. (2001). Daily air temperature and electricity load in Spain. *Journal of Applied Meteorology*, *40*(8), 1413–1421.
Ville de Montreal (2002). *Socioeconomic profile of city of Montreal*. Available at: http://ville. montreal.qc.ca/pls/portal/docs/page/librairie_fr/documents/28Montreal.pdf (retrieved).
Vörösmarty, C. J., Green, P., Salisbury, J., & Lammers, R. B. (2000). Global water resources: Vulnerability from climate change and population growth. *Science*, *289*(5477), 284–288.
Wake, B. (2013). Flooding costs. *Nature Climate Change*, *3*(9), 778.
Webster, P. J., Holland, G. J., Curry, J. A., & Chang, H. R. (2005). Changes in tropical cyclone number, duration, and intensity in a warming environment. *Science*, *309*(5742), 1844–1846.
Wheater, H., & Gober, P. (2013). Water security in the Canadian Prairies: Science and management challenges. *Philosophical Transactions of the Royal Society of London A: Mathematical, Physical and Engineering Sciences*, *371*(2002), 20120409.
Wheater, H. S., & Gober, P. (2015). Water security and the science agenda. *Water Resources Research*, *51*(7), 5406–5424.
Winslow, L. A., Read, J. S., Hansen, G. J., & Hanson, P. C. (2015). Small lakes show muted climate change signal in deepwater temperatures. *Geophysical Research Letters*, *42*(2), 355–361.
Wood, A. W., Leung, L. R., Sridhar, V., & Lettenmaier, D. P. (2004). Hydrologic implications of dynamical and statistical approaches to downscaling climate model outputs. *Climatic Change*, *62*(1), 189–216.
Zhao, H. X., & Magoulès, F. (2012). A review on the prediction of building energy consumption. *Renewable and Sustainable Energy Reviews*, *16*(6), 3586–3592.
Zimmerman, D., Pavlik, C., Ruggles, A., & Armstrong, M. P. (1999). An experimental comparison of ordinary and universal kriging and inverse distance weighting. *Mathematical Geology*, *31*(4), 375–390.